

HORNER METHOD APPLIED TO BUILDUP TESTS ON TRAVALE 22 WELL

A. Barelli, R. Celati, G. Manetti, and G. Neri*

Over a period of two years several Horner curves with different production times obtained from Travale 22 well were studied with a view to investigating the kind of boundary conditions existing in the reservoir.

Due to technical problems production history has often been very far from ideal, thus resulting in difficulties in analysis.

At fixed $1 + \frac{t}{\Delta t}$, P_D increases with an increase in t_{DA} , as expected for a well near impermeable boundaries, but all P_D approach zero when $\Delta t \rightarrow \infty$.

A contribution to pressure buildup from the boiling of a liquid phase cannot be excluded.

Travale 22 well was drilled in 1972 in Travale area, Tuscany, Italy, a few kilometers away from an area where some non-commercial wells had already been in existence for several years (Burgassi *et al.*, 1975).

This therefore was the first well to be drilled in the new area. During 1972 and 1973 there were several alternating periods of production and shut-in. Changes in production were often the result of technical problems and installation and maintenance operations so that the buildup data had to be gathered in non-ideal conditions.

Application of superposition principle

Several buildups are available from this period, with different production times, so that Horner plots

$$\frac{\pi h K M_w}{G_u z R T} (P_i^2 - P_w^2) \text{ vs. } \log \left(\frac{t + \Delta t}{\Delta t} \right)$$

with different "t" can be drawn.

A comparison between these curves and those taken from the available literature for many theoretical models (Figs. 1, 2, 3, 4, 5) can help towards an understanding of the nature, geometry and boundary conditions of the actual reservoir.

There is one difficulty when drawing these Horner plots for T22 well: P_i is not clearly determined in all the buildups, except for the first one. Every production period after this one began before shut-in pressure had stabilized so that the superposition principle must be applied.

*A. Barelli and G. Manetti, ENEL, Centro di Ricerca Geotermica, Pisa, Italy.
R. Celati, C.N.R., Istituto Internazionale per le Ricerche Geotermiche, Pisa.
G. Neri, ENEL, Gruppo Minerario Larderello, Italy.

Let us assume the existence of a function $P_D(t)$ that remains unchanged throughout exploitation. So we can write (Fig. 8)

$$p_i - p(\tau) = \frac{\mu}{2\pi kh} \sum_{j=1}^n \Delta q_j P_D(\tau - \tau_j) \quad (1)$$

where $\Delta q_1 = q_1$, $\Delta q_2 = q_2 - q_1$, ..., $\Delta q_j = q_j - q_{j-1}$, and τ_j is the moment when the flow rate changes to q_j .

If a logarithmic approximation for P_D is adequate, (1) becomes

$$p_i - p(\tau) = \frac{q_1 \mu}{4\pi kh} \sum_{j=1}^n \frac{\Delta q_j}{q_1} \ln(\tau - \tau_j)$$

and a classical semilogarithmic graph is obtained by plotting

$$\frac{4\pi kh}{q_1 \mu} (p_i - p(\tau)) \quad \text{vs.} \quad \sum_{j=1}^h \frac{\Delta q_j}{q_1} \ln(\tau - \tau_j)$$

For our system the validity of the logarithmic approximation was doubtful for the whole shut-in period (Figs. 6 & 7).

As we wanted to compare our T.22 Horner graphs with those available for theoretical cases, we tried a different approach.

Let us consider, as in Fig. 8, two consecutive shut-ins and let $p_{ext}(\tau)$ be the value assumed by the pressure if the first shut-in were to continue to time τ .

In this case we have

$$p_i - p(\tau) = \frac{\mu}{2\pi kh} \sum_{j=1}^n \Delta q_j P_D(\tau - \tau_j) \quad (2)$$

and

$$p_i - p_{ext}(\tau) = \frac{\mu}{2\pi kh} \sum_{j=1}^{n-2} \Delta q_j P_D(\tau - \tau_j) \quad (3)$$

Combining these two equations we obtain

$$p_{ext}(\tau) - p(\tau) = \frac{\mu}{2\pi kh} \sum_{j=n-1}^n \Delta q_j P_D(\tau - \tau_j) \quad (4)$$

or, if q is the last flow rate

$$\frac{2\pi kh}{8\mu} (p_{ext}(\tau) - p(\tau)) = P_D(t + \Delta t) - P_D(\Delta t) \quad (5)$$

with t and Δt defined in Fig. 8. For gas wells, eq 5 becomes

$$\frac{\pi kh M_w}{G \mu z R T} (p_{ext}^2(\tau) - p_{ws}^2(\tau)) = P_D(t + \Delta t) - P_D(\Delta t) \quad (6)$$

The theoretical Horner plot gives $P_D(t + \Delta t) - P_D(\Delta t)$ vs $\log(\frac{t + \Delta t}{\Delta t})$

If we are able to extrapolate the previous buildup curve so that a sufficiently approximate value is obtained for $p_{ext}(\tau)$, we can use the left hand side of eq. (6) to construct Horner plots from field data. These can then be compared with the available Horner plots of theoretical cases to obtain information on the most suitable model for the real situation.

Horner Plots for Travale 22 Well

The curves shown in Fig. 9 were plotted according to the above procedure. Some buildup curves were excluded there being no possibility of obtaining reliable values for $p_{ext}(\tau)$; for this same reason some other curves were shortened in their final part although further shut-in pressure data were available.

Production time t is reported as a parameter instead of t_{DA} as the hydraulic diffusivity and reservoir area are not known.

$$\text{The } kh \text{ value used to calculate } \frac{\pi h K M_w}{G \mu z R T} (p_{ext}^2 - p_{ws}^2$$

was obtained by conventional Horner plots and type-curve matching (Barelli et al. 1975).

Some very short delivery during long shut-ins and very short shut-ins during long production periods have been ignored.

From Fig. 9 we can observe that:

- there is a regular displacement of the curves changing t ;
this displacement is such that the dimensionless $\frac{t + \Delta t}{\Delta t}$ is an increasing function of t for any given $\frac{t + \Delta t}{\Delta t}$
- $(p_{ext} - p_{ws}) \rightarrow 0$ when $t \rightarrow \infty$.

This is not so clear in Fig. 9 as some curves are not complete, due to the difficulty in extrapolating the previous curve.

The trend to recovery of initial pressure is evident in Fig. 7 which represents a very long buildup occurring about nine months after well blow-out.

Similar results were found by Celati and Galardi (1975) with a simplified analysis, assuming for p_i a constant value or the maximum value reached in the last long buildup.

From a comparison of T 22 curves with the theoretical cases given in Figs. 1 to 5, we see that downward displacement is generally obtained as the effect of impermeable boundaries as in Fig. 1 and, for a limited range of t_{DA} in Fig. 3. The same kind of t -dependence of the curve position is obtained for an infinite reservoir with linear or radial discontinuity when the well is placed in the higher mobility zone. The limiting hypothesis of constant diffusivity throughout the reservoir was formed for these cases. The curves in Figs. 4 and 5 are the most similar to those of T 22, as they also have similar trends for $\Delta t \rightarrow \infty$. In the case of a closed reservoir the asymptotic values for $\Delta t \rightarrow \infty$ are positive, increasing with an increase in t and, in the case of recharge through a limited section in the boundary, the curves intersect one another in the final part of the buildup.

However, the latter effect is much less evident for smaller values of t , and in our case it could be masked by experimental errors and the fact that the curves are not generally extended to very long Δt values.

Discussion and Conclusion

Some hypotheses can be drawn from these observations, although the results are insufficient to draw definite conclusions.

From the geological point of view, Travale 22 is located in a structural high of the reservoir formation connected with the recharge area to the west and bounded on its N, E, S sides by faults; the latter lower than the reservoir formation and putting the upper part of the structure in lateral contact with impermeable formations.

Geological hydrological and chemical data, obtained from other wells in the zone, have shown:

- an interference between the vapor-dominated system feeding **T 22** and the water-dominated system in the old wells area,
- sudden decreases in permeability outside **T 22** area,
- a limited connection between the structural high and the deeper surrounding reservoir (Burgassi ~~et al.~~ 1975).

The hypothesis of a high permeability zone surrounded by lower permeability zones agrees both with the geological information available and the similarity between the curves of **T 22** well and those of Figs. 4 and 5. The theoretical case considers a linear or radial discontinuity, in mobility and a uniform diffusivity, whereas the actual situation, although not completely known, may certainly be considered rather more complex. The complex geometry may be responsible for the shape of the buildup curves. However, we consider it very likely that a contribution to the pressure buildup comes from the boiling of liquid water both on the boundary of, and inside, the vapor dominated zone.

The reduction in pressure can favor the infiltration of liquid water from the relatively cold boundaries toward the warmer parts of the reservoir.

These observations are based on two-dimensional models. As there are doubts as to the validity of purely radial flow models, a three-dimensional model is now being constructed.

For a quantitative comparison of the various models with the field data we are going to use log-log instead of conventional semi log Horner graphs. A match obtained with vertical displacement only will let us choose the most suitable family of curves and determine kh and t_{DA} .

Nomenclature

a = distance from well to the linear discontinuity
A = reservoir area
c = compressibility
Fs = storage capacity ratio
G = mass production rate
h = reservoir thickness
k = permeability
M = mobility ratio
Mw = molecular weight
p = pressure
 P_D = dimensionless pressure
 p_{ext} = extrapolated shut-in pressure
 p_i = initial pressure
 p_{ws} = shut-in pressure
q = volume production rate (reservoir condition)
R = gas law constant
t = production time
 t_D, t_{DA} = dimensionless time
T = absolute temperature
z = compressibility factor
 $\Delta p = p_i - p_{ws}$
At = shut-in time
 Φ = porosity
 μ = viscosity
 τ = time

References

Barelli, A., R. Celati, G. Manetti, G. Neri, "Build-up and back-pressure tests on Italian geothermal wells." Second Symposium on Development and Utilization of Geothermal Resources, San Francisco, CA., May 1975.

Bixel, H. C., B. K. Larkin, and H. K. van Poollen, "Effect of Linear Discontinuities on Pressure Build-up and Drawdown Behavior." J. Pet. Tech. (Aug., 1963)- 885-895.

Bixel, H. C. and H. K. van Poollen, "Pressure Drawdown and Buildup in the Presence of Radial Discontinuities." Paper SPE 1516 presented at 41st Annual SPE Fall Meeting, Dallas, Texas (Oct. 2-5, 1966).

Burgassi, P. D., R. Cataldi, A. Rossi, P. Squarci, G. Stefani, and L. Taffi, "Recent developments of geothermal exploration in Travale-Radicondoli area." Second Symposium on Development and Utilization of Geothermal Resources, San Francisco, CA., May 1975.

Celati, R., and L. Galardi, "Applicazione del metodo di Horner alle curve di risalita del pozzo Travale 22." Unpublished report, Istituto Internazionale per le Ricerche Geotermiche, Pisa, 1975.

Ramey, H. J., Jr., and W. M. Cobb, "A general pressure buildup theory for a well in a square drainage area." J. Pet. Tech. (Dic. 1971), 1493-1505.

Ramey, H. J., Jr., A. Kumar, M. S. Gulati, "Gas well test analysis under water-drive conditions." American Gas Association, Arlington, Va. (1973), 312 pp.

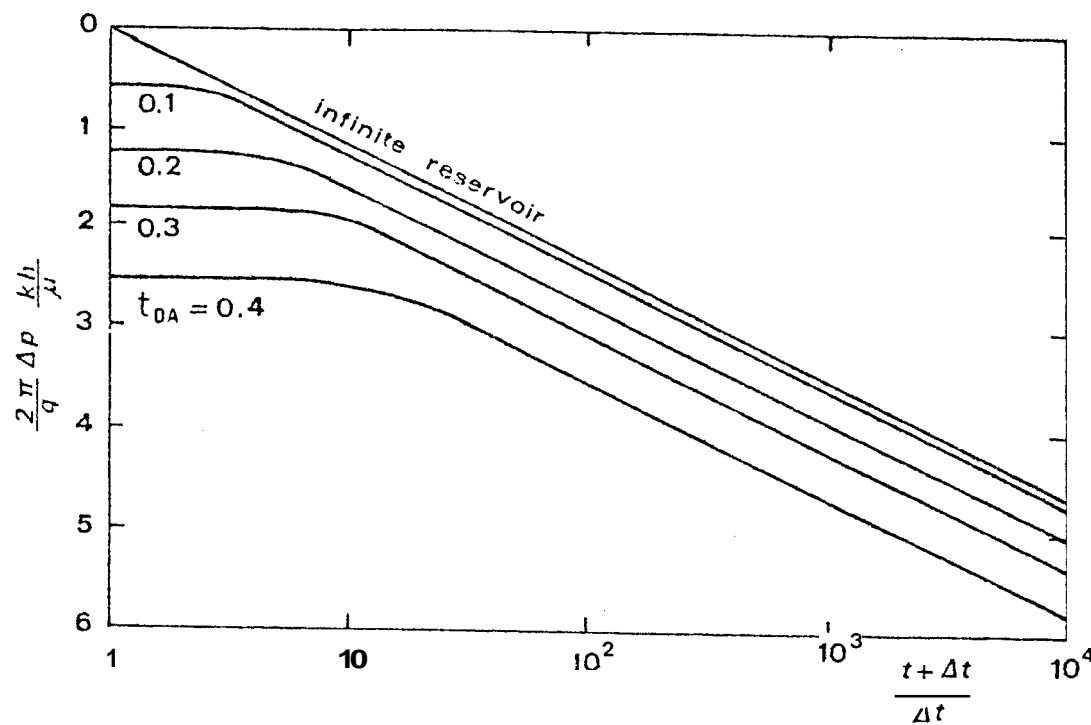


Fig. 1 - Horner plot for a well in the centre of a closed square.

$$t_{DA} = \frac{Kt}{\Phi \mu c A} \quad \text{--- (Ramey et al., 1971).}$$

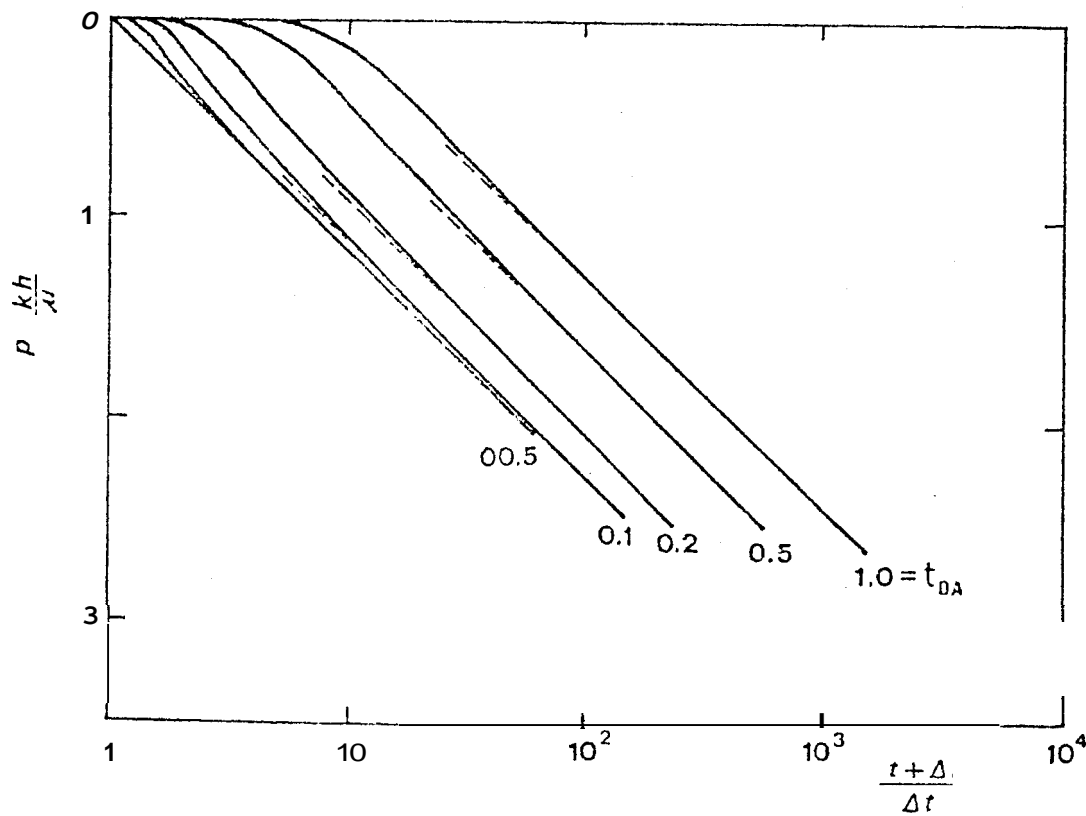


Fig. 2 - Horner plot for a well in the centre of a constant pressure square

$$t_{DA} = \frac{Kt}{\Phi \mu c A} \quad \text{--- (Ramey et al., 1973).}$$

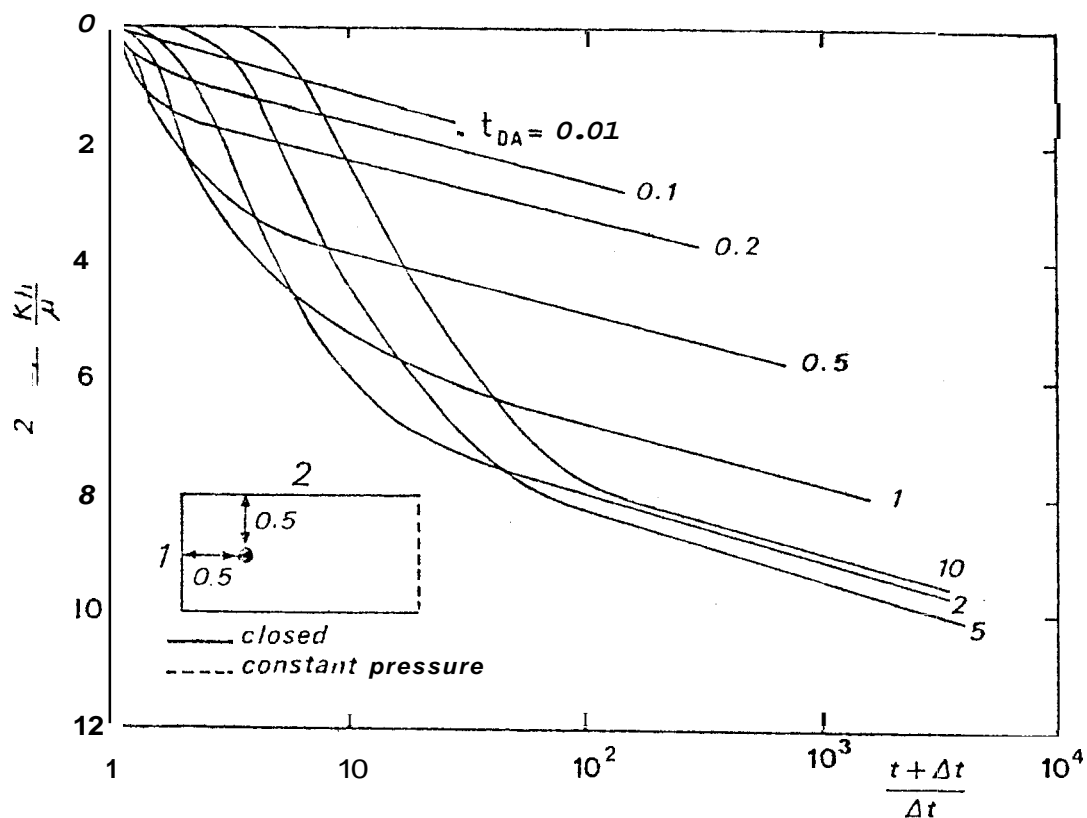


Fig. 3 - Horner plot for a well in a 2 : 1 rectangle with one short side at constant pressure (well position: see fig., $t_{DA} = \frac{Kt}{\phi \mu c A}$)
(Ramey *et al.*, 1973).

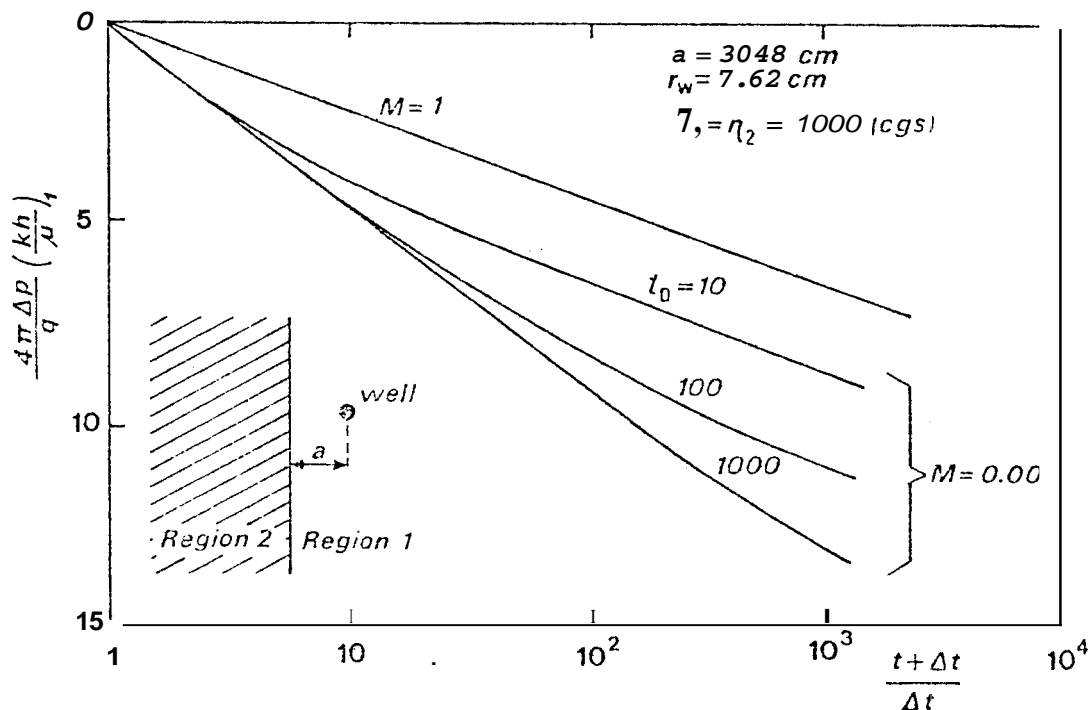


Fig. 4 - Horner plot for linear discontinuity case (Bixel *et al.*, 1963)
 $(t_{DA} = \frac{K_1 t}{\phi_1 \mu c_1 \gamma_1^2} ; M = \frac{(K/\mu)_2}{(K/\mu)_1})$.

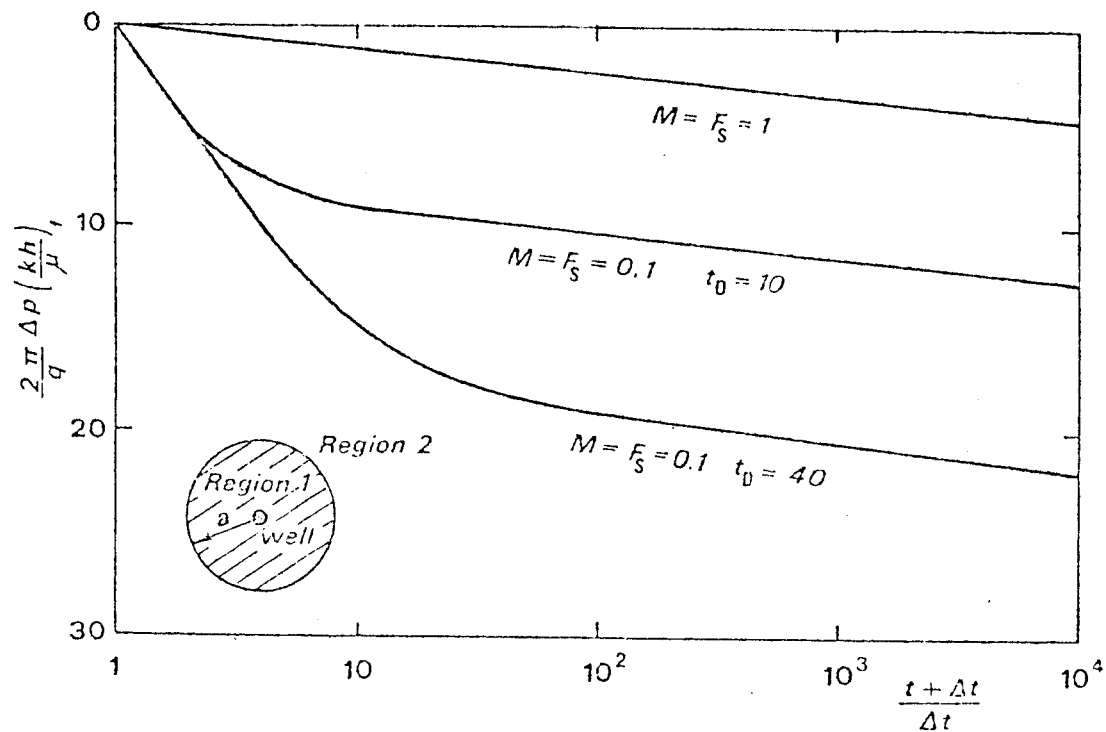


Fig. 5 - Horner plot for radial discontinuity case (Bixel et al., 1966)

$$(t_D = \frac{K_1 t}{\Phi_1 \mu c_1 D^2}; M = \frac{(k/\mu)_2}{(k/\mu)_1}; F_S = \frac{(\Phi c)_2}{(\Phi c)_1})$$

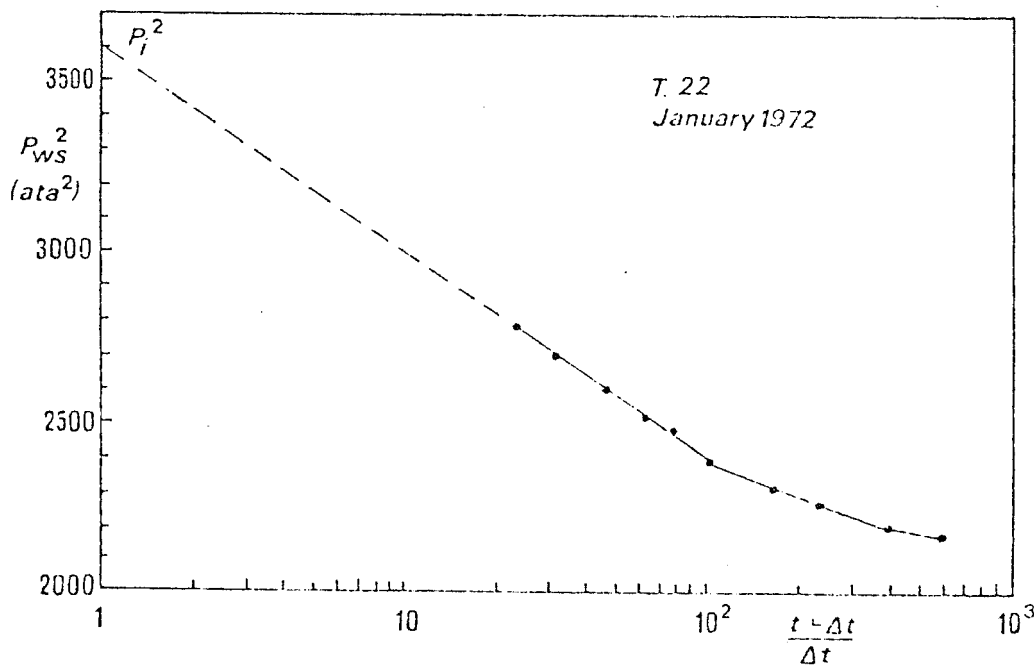


Fig. 6 - First shut-in curve for T 22 well.

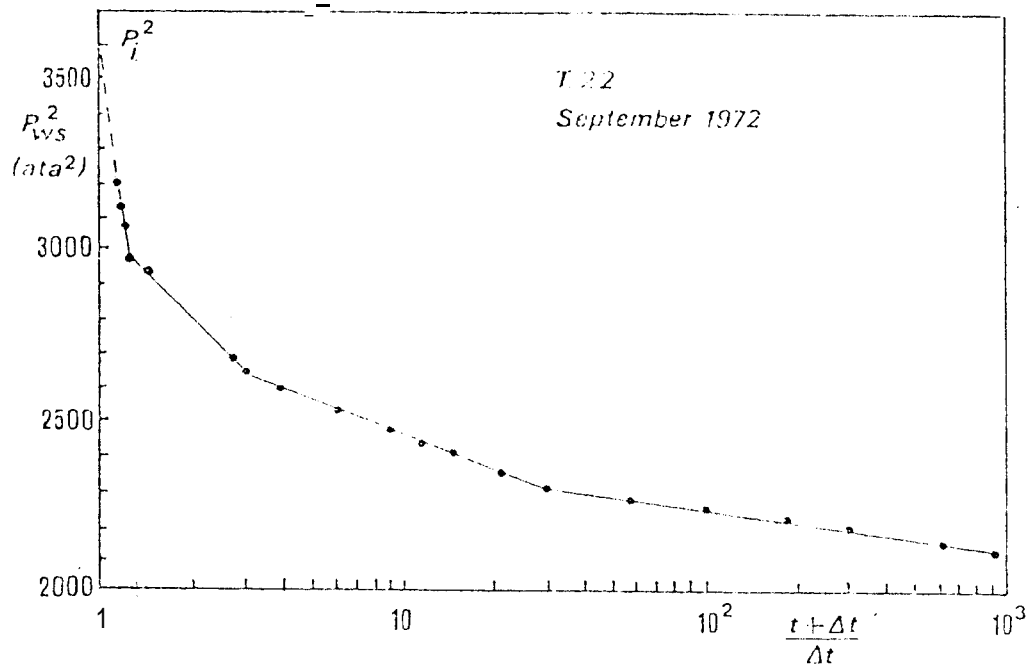


Fig. 7 - Shut-in curve for T 22 well.

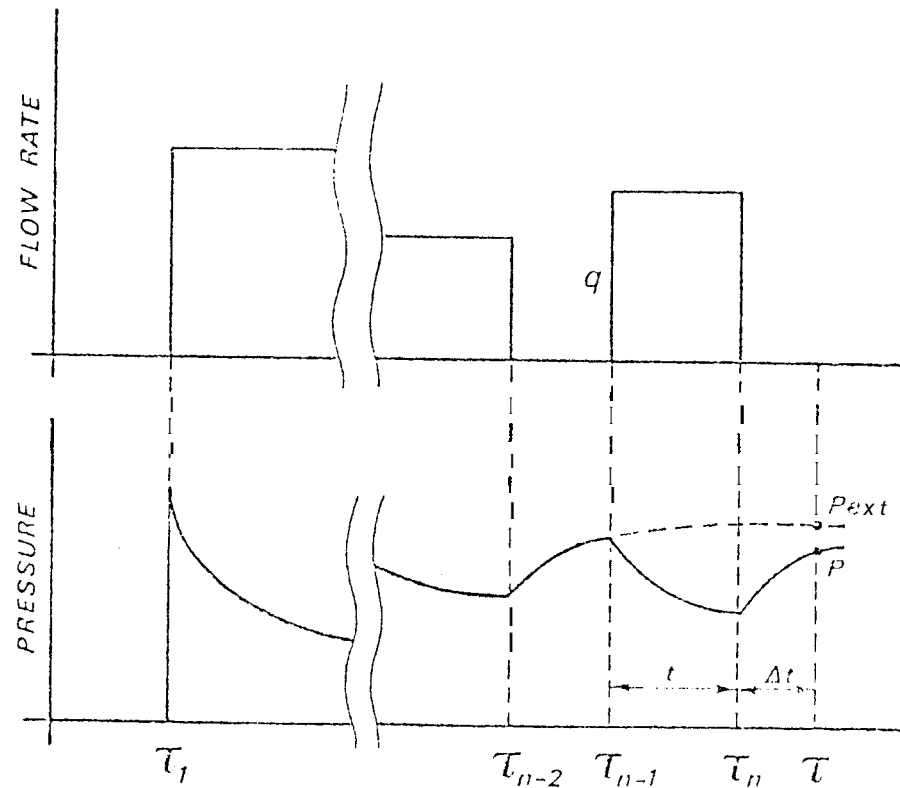


Fig. 8 - Design showing application of superposition principle.

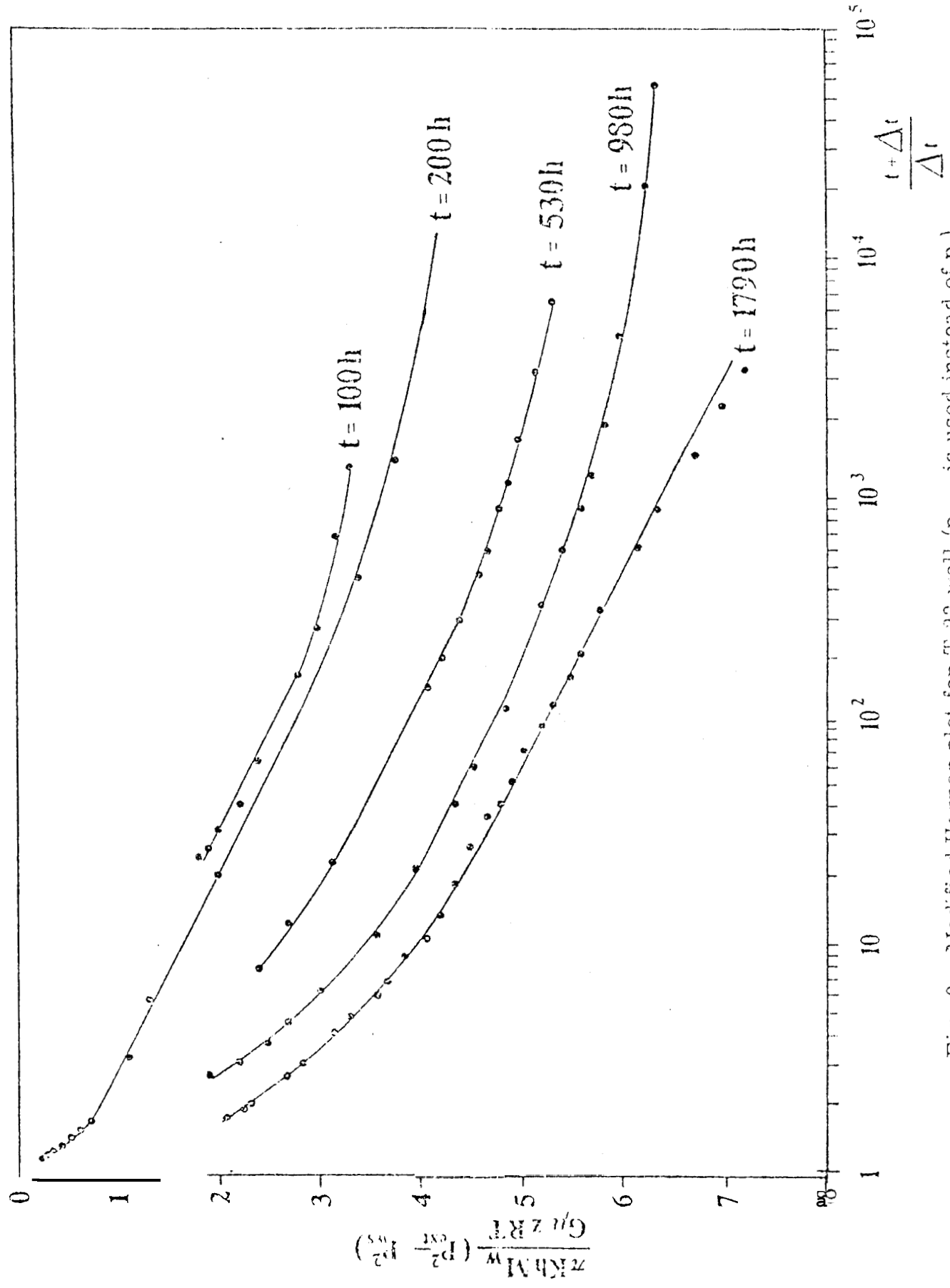


Fig. 9 - Modified Horner plot for T 22 well (P_{ext} is used instead of P_i).